

Highly Efficient Technique for the Full-Wave Analysis of Circular Waveguide Filters Including Off-Centered Irises

Ángel A. San-Blas and José M. Roca

Department of Communications Engineering
Miguel Hernández University of Elche, Elche, Spain
aasanblas@umh.es, jose.roca01@alu.umh.es

Abstract — A rigorous method for the full-wave analysis and design of waveguide filters implemented in circular waveguide technology, and including off-centered circular irises, is presented. The implemented tool is based on an integral equation technique, which provides a full-wave representation of the elementary blocks of the analyzed components in terms of generalized impedance matrices. With the aim of improving the efficiency of the developed tool, the radial variation of the modal solutions of the circular waveguides has been expressed in terms of sinusoidal functions, thus avoiding the use of the more cumbersome Bessel's functions employed in the classical formulation. Furthermore, line integrals have been used (instead of surface integrals) to compute the modal coupling coefficients of the planar waveguide junctions involved in the considered filters, thus drastically reducing the CPU effort related to the implemented tool. New designs concerning band-pass filters including off-centered circular irises are also provided. The obtained results show that the relative position of the considered circular irises can be considered as a new design parameter with a noteworthy influence on the electrical response of the investigated components. The accuracy of the proposed method has been successfully validated by comparing the obtained results with data extracted from both the technical literature and a commercial software based on the finite-element method.

Index Terms — Circular waveguide filters, integral equation technique, multimode equivalent network, off-centered irises.

I. INTRODUCTION

Circular waveguides are widely used in the fabrication of many passive and active components (such as waveguide filters [1], traveling-wave tubes [2], orthomode transducers [3] and turnstile junctions [4]), and they can be considered as key elements of current space communications devices in both microwave and millimeter-wave range [5-8]. Furthermore, the consideration of off-centered irises in circular waveguide filters is an

important topic in the design of a great variety of microwave components, since off-centered irises can provide a new design parameter (i.e., the relative position of the iris), thus allowing a more flexible computer-aided design process. The main motivation of this work is that, to the authors' knowledge, very few works concerning the full-wave analysis of circular waveguide filters, including off-centered circular irises, can be found in the technical literature. Besides, a common feature of such technical contributions is that they are not focused on developing efficient analysis tools from a computational point of view. For instance, the analysis method proposed in [9-10] is based on the conservation of the complex power technique, which employs the more cumbersome Bessel's functions to express the modal solutions of the circular waveguides, and also to compute the modal coupling coefficients of the analyzed planar junctions. Moreover, in contrast to the procedure used in the present work, such modal coupling coefficients are computed in [9-10] by using surface integrals instead of line integrals. Therefore, an increased CPU-effort may be expected in the solutions proposed in the aforementioned contributions. In addition, the modal method used in [9-10] assumed that no propagation modes exist in the smaller circular waveguide, thus limiting the validity of such model to a narrow frequency range.

Another contribution based on the least-squares boundary residual method was proposed in [11] to analyze thick eccentric circular irises in circular waveguides. However, the technique used in such work also resorts to computing surface integrals in order to analyze the planar junction, and the convergence of the obtained results depends on selecting very large dimensions for the computed matrices. Moreover, the authors of [11] reported a loss of accuracy at high frequencies values. A very recent work has been presented in [12], where complex discontinuities in circular waveguides are analyzed. Nevertheless, such work is based on a hybrid approach combining the finite-element method and a multimode variational technique, thus requiring higher CPU resources than the

approach proposed in the present work. In fact, the authors of [12] state that the simulation of a single circular discontinuity needs “few minutes” ([12], p. 103) using a CPU very similar to the one employed in this work. For comparison purposes, it is worth mentioning that the simulation tool developed in the present work is able to perform the overall analysis of a circular waveguide filter (composed of several discontinuities) in just few seconds.

Although other analysis methods based on numerical techniques (as the finite-element method) can be employed to analyze circular waveguide filters, such techniques typically use high CPU resources (both time and memory), since the whole analyzed structure needs to be meshed to achieve an electromagnetic characterization of the component.

In order to overcome all cited drawbacks of the aforementioned contributions, the main objective of this work is to present a novel and very efficient approach for the rigorous full-wave analysis of waveguide filters composed of the cascade connection of circular waveguides of different radii, and considering the inclusion of off-centered circular irises (see Fig. 1). The influence of the off-centered circular irises in the electrical response of different waveguide filters is investigated, and some useful guidelines for microwave designers are provided (i.e., the relative position of the circular irises can be considered as an important new design parameter). The implemented tool is based on an integral equation technique, which provides a full-wave representation of a planar junction between two off-centered circular waveguides in terms of a generalized impedance matrix [13]. This technique is very efficient from a computational point of view and provides a wide-band characterization of the waveguide planar junctions present in the considered device.

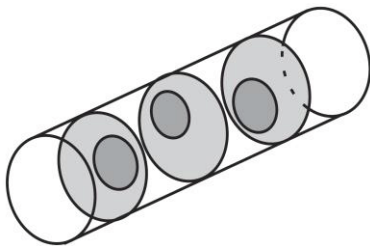


Fig. 1. Waveguide filter composed of the cascade connection of 7 circular waveguides. Note that the circular waveguides of smaller cross-section represent the waveguide irises of the filter and they are off-centered with respect to the axis of the filter. The length of the waveguide irises is small compared to the length of the resonators.

With the aim of optimizing the computational efficiency of the implemented tool, we follow a new

procedure in which the radial variation of the modal solutions of the circular waveguides is expressed in terms of sinusoidal functions, thus avoiding the use of the more cumbersome Bessel’s functions employed in the classical formulation. Furthermore, the surface integrals that must be calculated to compute the modal coupling coefficients between the two circular waveguides involved in the considered planar junctions are transformed into line integrals, thus reducing even more the CPU effort of the method. Additionally, the solution of the banded linear system obtained after performing the cascade connection of the derived wide-band matrices has been carried out by means of an iterative technique very efficient from a computational point of view. As a result, this novel approach produces a substantial improvement in terms of reduction of the computational effort with respect to previous works on the same subject.

In order to validate the proposed method, several band-pass circular waveguide filters including off-centered irises are analyzed and designed. The obtained simulated results are successfully compared to numerical data extracted from both the technical literature and a commercial tool based on the finite-element method, thus demonstrating the accuracy of the implemented software tool.

II. FULL-WAVE ANALYSIS OF CIRCULAR WAVEGUIDE FILTERS INCLUDING OFF-CENTERED IRISES

Waveguide filters based on off-centered circular irises can be readily analyzed by means of the so-called segmentation technique [14], which consists of decomposing the analysis of a complete waveguide structure into the characterization of its elementary key building blocks. In our particular case, a waveguide filter can be described as the cascade connection of planar junctions between off-centered circular waveguides, and uniform sections of circular waveguides, as it is shown in Fig. 1.

Both types of the aforementioned key building blocks can be characterized in terms of equivalent wide-band matrices. On the one hand, the electromagnetic characterization of a planar junction between two off-centered circular waveguides has been carried out by implementing the integral equation technique described in [13], which provides a full-wave characterization of the discontinuity in terms of an equivalent generalized impedance matrix (GIM) in the form:

$$Z_{(m,n)}^{(\xi,\gamma)} = \begin{cases} \sum_{q=1}^Q \alpha_q^{(n,\gamma)} A_{m,q}^*, & \text{if } \xi = 1 \\ \alpha_m^{(n,\gamma)} & \text{if } \xi = 2 \end{cases}, \quad (1)$$

where $(\xi, \gamma) = 1, 2$ denotes the two ports of the junction; $A_{m,q}$ represents the modal coupling coefficients

between two modes (m -th and q -th) of the circular waveguides involved in the junction; $\alpha_q^{(n,\gamma)}$ is a set of expansion coefficients used to represent the transversal magnetic field in the plane of the junction, and Q is the number of the considered expansion coefficients (the details of this formulation can be found in [13]). The multimode equivalent representation of the planar waveguide junction in terms of the GIM derived in (1) has been depicted in Fig. 2. In this figure, $I_i^{(\xi)}$ and $V_i^{(\xi)}$ (with $\xi=1,2$) are the corresponding modal currents and modal voltages, respectively; $\bar{I}_i^{(\xi)}$ represents a set of auxiliary modal currents; $N^{(\xi)}$ is the number of considered accessible modes, and $\hat{Y}_i^{(\xi)}$ are the so-called asymptotic admittances, which represent the modal admittance of high-order modes and are defined as follows:

$$\hat{Y}_i^{(\xi)} = \begin{cases} -j \frac{k_{t,i}^{(\xi)}}{\omega\mu}, & \text{if } i \text{ is a TE mode} \\ j \frac{\omega\epsilon}{k_{t,i}^{(\xi)}}, & \text{if } i \text{ is a TM mode} \end{cases}, \quad (2)$$

where $\omega = 2\pi f$, and $k_{t,i}^{(\xi)}$ is the cut-off wavenumber related to the i -th mode of the circular waveguide considered at port (ξ).

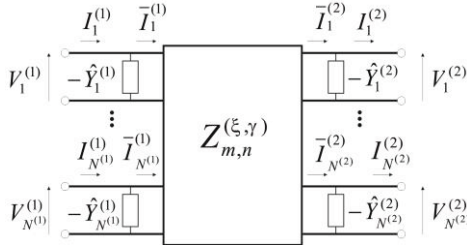


Fig. 2. Multimode equivalent representation of a planar waveguide junction in terms of a generalized impedance matrix.

The main advantage of this technique lies in its high computational efficiency, due to the fact that the size of the obtained GIM only depends on the number of the so-called accessible modes ($N^{(1)}$ and $N^{(2)}$ in Fig. 2), which is usually low to reach convergent results (10-20 modes in most cases). Moreover, since the frequency dependence of the obtained integral equation can be extracted from the kernel of such equation, the efficiency of the technique gets increased [13].

In order to obtain the elements of the GIM related to each planar junction, the modal coupling coefficients between the two circular waveguides involved in the discontinuity must be calculated first as follows:

$$A_{m,q} = \iint_S \mathbf{h}_m^{(1)}(\rho, \phi) \cdot \mathbf{h}_q^{(2)}(\rho, \phi) dS, \quad (3)$$

where $\mathbf{h}_\delta^{(i)}(\rho, \phi)$ with ($\delta = m, q$) is the magnetic vector mode function related to the δ -th mode of the i -th waveguide ($i=1,2$), and ρ and ϕ are the classical cylindrical coordinates. It is important to emphasize that the calculation of the coupling integral $A_{m,q}$ constitutes the core of the method. In fact, once these coupling coefficients are calculated, the computation of the GIM related to the planar waveguide junction can be easily performed following the general method detailed in [13].

Furthermore, it is important to note that the previous Equation (3) entails a surface integral that must be evaluated in the cross-section of the smaller circular waveguide of the junction. However, in virtue of the theory developed in [15], such surface integral can be transformed into a line integral, thus improving the CPU effort of the implemented tool. This transformation is very important from a computational point of view, since all the calculations involved in the evaluation of the coupling integral (3) must be performed using numerical methods. Therefore, following the guidelines of the work presented in [15], the evaluation of the previous modal coupling coefficients can be expressed in terms of line integrals as follows:

$$A_{m_{TE},q_{TE}} = \frac{k_{t,q}^2}{k_{t,q}^2 - k_{t,m}^2} \oint_c \frac{\partial \psi_m^{TE}(\rho, \phi)}{\partial \rho} \chi_q^{TE}(\rho, \phi) \rho d\phi, \quad (4)$$

$$A_{m_{TE},q_{TM}} = 0, \quad (5)$$

$$A_{m_{TM},q_{TE}} = \oint_c \frac{\partial \psi_m^{TM}(\rho, \phi)}{\partial \phi} \chi_q^{TE}(\rho, \phi) d\phi, \quad (6)$$

$$A_{m_{TM},q_{TM}} = -\frac{k_{t,m}^2}{k_{t,q}^2 - k_{t,m}^2} \oint_c \frac{\partial \chi_q^{TM}(\rho, \phi)}{\partial \rho} \psi_m^{TM}(\rho, \phi) \rho d\phi, \quad (7)$$

where $k_{t,m}$ represents the cut-off wavenumber related to the m -th mode of the bigger circular waveguide of the junction; $k_{t,q}$ is the corresponding cut-off wavenumber associated to the q -th mode of the smaller circular waveguide; $\psi_m(\rho, \phi)$ is the normalized scalar potential related to the m -th mode of the bigger circular waveguide, and $\chi_q(\rho, \phi)$ is the normalized scalar potential related to the q -th mode of the smaller circular waveguide. Note that the previous expressions derived in (4)-(7) for the calculation of the coupling integral (3) depend on the type of the involved modes (i.e., TE or TM modes).

To evaluate the modal coupling coefficients using line integrals, the TE and TM normalized scalar potentials of a circular waveguide are, therefore, needed. To this aim, in this work we follow a new procedure based on expressing the radial variation of the modal solutions in terms of sinusoidal functions [16]. Proceeding in this way, the CPU effort related to

the calculation of the modal coupling coefficients is substantially reduced, since we do not need to deal with the more cumbersome Bessel's functions employed in the classical formulation. The expressions of the normalized modal potentials (TE and TM) can be obtained as:

$$\psi_m^{\text{TE}}(\rho, \phi) = N_m^{\text{TE}} \left\{ \sum_{n=0}^P d_m^{(n)} \sin\left(\pi(n+0.5)\frac{\rho}{R}\right) \right\} \Phi_s(\phi), \quad (8)$$

$$\psi_m^{\text{TM}}(\rho, \phi) = N_m^{\text{TM}} \left\{ \sum_{n=1}^P d_m^{(n)} \sin\left(n\pi\frac{\rho}{R}\right) \right\} \Phi_s(\phi), \quad (9)$$

where R is the radius of the considered circular waveguide; N_m is the normalization factor related to the m -th mode; $d_m^{(n)}$ is the set of eigenvectors that describe the radial variation of the m -th mode; s is the angular modal index related to the m -th mode; $\Phi_s(\phi) = \cos(s\phi)$ or $\sin(s\phi)$ depending on the parity of the mode, and P is the number of terms considered in the radial expansion. If the angular modal index s is equal to zero, the following expressions must be used:

$$\psi_{m,(s=0)}^{\text{TE}}(\rho) = N_{m,(s=0)}^{\text{TE}} \sum_{n=0}^P d_m^{(n)} \cos\left(n\pi\frac{\rho}{R}\right), \quad (10)$$

$$\psi_{m,(s=0)}^{\text{TM}}(\rho) = N_{m,(s=0)}^{\text{TM}} \sum_{n=0}^P d_m^{(n)} \cos\left(\pi(n+0.5)\frac{\rho}{R}\right), \quad (11)$$

where $N_{m,(s=0)}$ is the corresponding normalization factor.

Next, we need to define a common reference system in order to carry out the computation of the modal coupling coefficients. To this end, the axis system depicted in Fig. 3 has been used. In such figure, the coordinates (ρ_0, ϕ_0) are used to express the offset of the center of the smaller waveguide with respect to the center of the bigger waveguide, while (ρ, ϕ) and (ρ_1, ϕ_1) are the local reference systems used in the bigger and smaller circular waveguides, respectively.

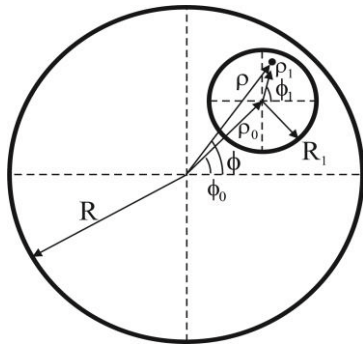


Fig. 3. Reference system used for the analysis of a planar junction between two off-centered circular waveguides.

Since the line integrations (4)-(7) have to be performed over the contour of the smaller circular waveguide, we are interested in expressing the local coordinates (ρ, ϕ) of the bigger waveguide in terms of the local coordinates (ρ_1, ϕ_1) of the smaller waveguide. Therefore, starting from Fig. 3, it is possible to state:

$$\rho = \sqrt{\rho_0^2 + \rho_1^2 + 2\rho_0\rho_1 \cos(\phi_1 - \phi_0)}, \quad (12)$$

$$\phi = \arctan\left(\frac{\rho_0 \sin(\phi_0) + \rho_1 \sin(\phi_1)}{\rho_0 \cos(\phi_0) + \rho_1 \cos(\phi_1)}\right). \quad (13)$$

Afterwards, we can use the transformations derived in (12)-(13) to update the expressions (8)-(11) related to the normalized modal potentials of the bigger circular waveguide. The normalized modal potentials of the smaller waveguide can be readily obtained starting from Equations (8)-(11), by using the local coordinates (ρ_1, ϕ_1) and denoting as R_1 the radius of the waveguide. In the end, the required modal coupling coefficients derived in (4)-(7) can be computed using classical numerical techniques, and the corresponding GIM of the planar junction can be finally calculated by means of expression (1).

Once the expressions of the wide-band matrices related to the planar waveguide junctions have been derived using the proposed technique, next step consists of characterizing the uniform waveguide sections present in the component. To this aim, let us consider the structure represented in Fig. 4, where we have illustrated a section of an arbitrary filter composed of the cascade connection of 3 circular waveguides of different radii. Note that the different planar waveguide junctions have been highlighted using dashed lines on the upper side of Fig. 4. In this figure, we have represented the multimode equivalent representation of such structure in terms of the computed GIMs $Z_{m,n}^{\text{PWJ1}}$ and $Z_{m,n}^{\text{PWJ2}}$, which are both associated to the planar waveguide junctions. We have also included in Fig. 4 the corresponding uniform waveguide section of length l used to interconnect the circular waveguides of greater radius.

Our objective is to obtain a multimode equivalent representation ($Z_{m,n}^{\text{UWS}}$ in Fig. 4) of the uniform waveguide section of length l , while also taking into account the asymptotic admittances introduced by the integral equation technique (see the dashed lines on the lower side of Fig. 4). To this aim, we should first obtain an equivalent lumped pi-network representation for the uniform waveguide section of length l and, afterwards, take into consideration the asymptotic admittances represented in Fig. 4. Proceeding in this way, the following generalized impedance matrix can be readily computed:

$$Z_{m,n}^{UWS} = \begin{pmatrix} Y^{(a)} & Y^{(b)} \\ Y^{(b)} & Y^{(c)} \end{pmatrix}^{-1}, \quad (14)$$

where $Y^{(a)}$, $Y^{(b)}$ and $Y^{(c)}$ are diagonal matrices whose non-zero elements can be written as:

$$Y_i^{(a)} = jY_{0,i} (\tan(\beta_i l / 2) - \csc(\beta_i l)) - \hat{Y}_{i,PWJ1}^{(2)}, \quad (15)$$

$$Y_i^{(b)} = -jY_{0,i} \csc(\beta_i l), \quad (16)$$

$$Y_i^{(c)} = jY_{0,i} (\tan(\beta_i l / 2) - \csc(\beta_i l)) - \hat{Y}_{i,PWJ2}^{(1)}, \quad (17)$$

with $i=1,2,\dots,N$, being N the number of considered accessible modes. In the previous Equations (15)-(17), $Y_{0,i}$ is the modal characteristic admittance related to the i -th mode of the considered waveguide section, and β_i is the corresponding propagation constant.

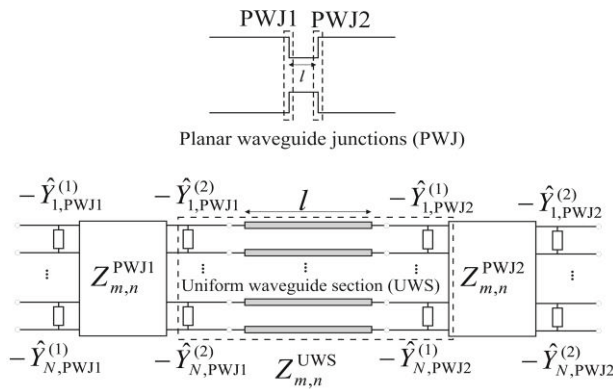


Fig. 4. Section of an arbitrary circular waveguide filter. Multimode equivalent network representation in terms of the obtained generalized impedance matrices (GIM). Note that N accessible modes are considered, and a uniform circular waveguide section of length l is included between the two GIMs.

Once the expressions for the wide-band matrices of all the elementary blocks of the structure (i.e., planar waveguide junctions and uniform waveguide sections) have been derived using the proposed techniques, the cascade connection of the obtained generalized impedance matrices must be performed in order to compute the electrical response of the whole filter. In relation to this, a very important advantage derived from expressing the GIM related to the uniform waveguide sections in the way we have previously described, is that the cascade connection of the obtained wide-band matrices produces a banded linear system (the non-zero coefficients of the matrix are distributed

over its main diagonals), which can be efficiently solved by means of an iterative technique. In fact, the banded configuration of such linear system can be exploited to perform an efficient inversion of the coefficients matrix following the guidelines proposed in [17] (although the procedure described in [17] is applied for the connection of generalized admittance matrices, it has been properly extended to cope with the cascade connection of generalized impedance matrices).

III. RESULTS AND DISCUSSION

The objective of this section is to validate the implemented tool for the full-wave analysis of waveguide filters based on off-centered circular irises. In order to obtain convergent results in the performed simulations, only 15 accessible modes have been used in all circular waveguides, and $P=150$ terms have been required in the radial expansions of the expressions (8)-(11). In addition, it is important to point out that the implemented tool is able to detect the presence of identical planar junctions in the filter to avoid unnecessary calculations (such detection is specially important in the case of symmetrical filters). Furthermore, if the circular irises of the filter are all in a centered position, note that only $TE_{1,r}$ and $TM_{1,r}$ modes are excited, and the developed tool is able to exploit this fact to reduce the overall CPU effort.

Firstly, we proceed to validate the proposed tool by analyzing a band-pass waveguide filter designed in [1], which makes use of centered circular irises (note that the method proposed in [1] can deal only with filters including centered irises). In this particular case, since the component does not include off-centered irises, the offset value is $\rho_0 = \phi_0 = 0$ (see Fig. 3). The analyzed filter is composed of the cascade connection of 7 circular waveguides, and its geometry and dimensions can be found in [1] (page 1140, Fig. 1). The radii (mm) of the waveguides are (numbered from left to right, according to Fig. 1): $R_1 = R_7 = 6.985$ (input and output waveguides), $R_3 = R_5 = 6.985$ (resonators), $R_2 = R_6 = 4.34$ and $R_4 = 3.51$ (irises). The length of the two resonators is 18.7 mm, and the thickness of the irises is 0.1 mm. This filter has been simulated using the implemented tool and the obtained scattering parameters are presented in Fig. 5. In this figure, our results are successfully compared with the data presented in the technical literature [1]. With regard to the computational efficiency of the developed tool, it is worth mentioning that the electrical response was computed in just 0.06 seconds per frequency point (Intel Core i3@3.1 GHz - 4 GB RAM).

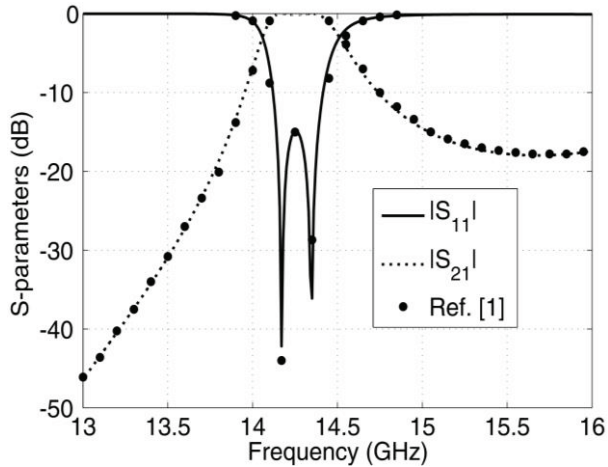


Fig. 5. S-parameters (dB) of a circular waveguide filter composed of 7 waveguides. The circular irises are all in a centered position. The obtained results are compared with the data extracted from the technical literature [1].

Next, we investigate the effect of considering off-centered circular irises in the structure. To this aim, we start from the filter analyzed in Fig. 5, and we proceed to off-center the circular irises of the component in order to study the influence of such variation on the electrical response of the device. Although, in this case, the three irises of the filter have been off-centered in the same magnitude, note that the implemented tool can deal with arbitrary off-centered irises, so there is no restriction in assigning a different offset to each circular iris. Figure 6 shows the electrical response of the filter for different values of the considered offset ρ_0 (mm), ϕ_0 (rad). The electrical response of the filter with centered irises (blue solid curve) has also been included in Fig. 6. Moreover, we have successfully compared the results of our simulation tool for the general case $\rho_0 = 2.343$ mm, $\phi_0 = 0.876$ rad (grey solid curve) with the simulated data provided by a commercial simulation tool (Ansoft HFSS 12) based on the finite-element method (FEM), thus fully validating the accuracy of the proposed technique. The results presented in Fig. 6 have been calculated in just 0.09 seconds per frequency point.

With regard to the parametric study performed in Fig. 6, it is important to point out that, compared to the filter with centered irises (blue solid curve), the electrical response of the component hardly change when different values of ρ_0 are considered along the line $\phi_0 = \pi/2$ rad (vertical displacement of the center of the iris). In fact, we observe that the electrical response for the case $\rho_0 = 2.25$ mm, $\phi_0 = \pi/2$ rad,

only has experienced a frequency shift, preserving both a good reflection level and the original relative bandwidth. As a consequence, these results show that the relative position of the circular iris can be considered as an additional design parameter to easily achieve a frequency shift of the electrical response of the device.

However, when different values of ρ_0 are considered along the line $\phi_0 = 0$ rad (horizontal displacement of the center of the iris), a severe degradation of the passband of the filter may be expected, specially when high values of ρ_0 are considered (see, for instance, the red solid curve in Fig. 6). The same behavior can be observed for a general displacement of the center of the circular iris (see grey solid curve in Fig. 6). Therefore, in general terms, we conclude that a degradation of the electrical response of the filter may be expected when it has been specifically designed with centered circular irises.

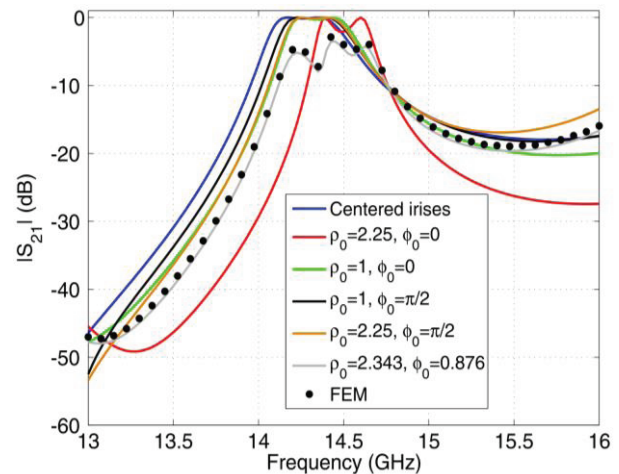


Fig. 6. Transmission parameters (dB) of the waveguide filter analyzed in Fig. 5 considering off-centered circular irises.

Finally, we present in Fig. 7 a new design of a Ku-band band-pass filter implemented in circular waveguide technology (composed of the cascade connection of 7 waveguides), including off-centered circular irises. A simple custom code based on the minimization of the average return losses has been developed in order to design the filter. In this design, the three irises of the structure have been off-centered using different offset values. The considered offsets have been listed in Table 1, while the radii and lengths of the circular waveguides are shown in Table 2 (the waveguides and irises have been numbered from left to right, according to Fig. 1).

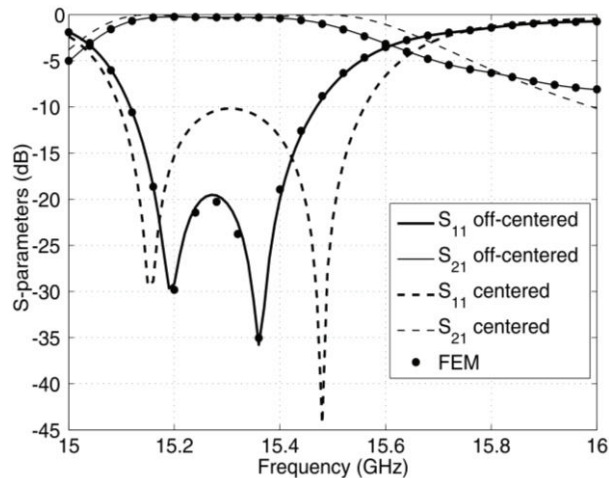


Fig. 7. Design of a band-pass filter including off-centered circular irises. The electrical performance of the designed filter (solid curves) is compared with the case where centered circular irises are used (dashed curves). Simulated data obtained using a commercial software based on the finite-element method (FEM) are also included to validate the proposed method.

Table 1: Offsets of the irises considered in the band-pass filter designed in Fig. 7

Irish	ρ_0 (mm)	ϕ_0 (rad)
1	2.485	1.367
2	2.711	1.549
3	2.208	1.311

Table 2: Radii and lengths of the circular waveguides of the band-pass filter designed in Fig. 7

Waveguide	Radius (mm)	Length (mm)
1	6.985	10.0
2	3.946	0.1
3	6.985	14.541
4	3.208	0.1
5	6.985	14.525
6	3.968	0.1
7	6.985	10.0

It is worth noting that the band-pass filter designed in Fig. 7 presents an improved electrical response with respect to the filter designed in [1] (see Fig. 5), which operates at the same frequency band and makes use of the same number of circular waveguides (employing centered irises). In this case where off-centered irises have been employed, we have achieved a reflection level under -20 dB in the whole passband (about 250 MHz) of the filter, thus proving that the relative position of the iris can be considered as a new design parameter. We have also compared the results of our simulation

tool (off-centered case) with the simulated data provided by Ansoft HFSS, and an excellent agreement can be observed, thus fully validating the accuracy of the proposed modal technique.

Moreover, we have also included in Fig. 7 (using dashed lines) the electrical response of the new designed filter, but this time considering centered irises. It can be observed that the filter based on off-centered irises provides an improved electrical performance compared to the filter based on centered irises, thus demonstrating that the relative position of the iris has a noteworthy influence on the design process.

It is important to mention that the overall analysis of the new designed filter (off-centered case) only needed 0.12 seconds per frequency point. In contrast, the simulation performed using the commercial tool based on the finite-element method needed 2.3 seconds per frequency point (almost 20 times slower). Moreover, the hybrid analysis method presented in [12] needs few minutes to analyze just one planar junction between two circular waveguides. Therefore, the developed software achieves a substantial improvement in terms of reduction of the computational effort with respect to other analysis techniques, so it can be employed for design purposes employing very low CPU resources.

IV. CONCLUSION

A rigorous method for the full-wave analysis of circular waveguide filters including off-centered irises has been proposed. The implemented tool is based on an integral equation technique, and makes use of the segmentation method to provide a rigorous electromagnetic characterization of all the elementary blocks involved in the analyzed filters in terms of generalized impedance matrices. The presented technique, which is very efficient from a computational point of view compared to other technical contributions on the same subject, has been successfully validated through the analysis and design of different band-pass waveguide filters with centered and off-centered circular irises. The obtained results show that the relative position of the circular waveguide irises can be considered as a new design parameter having a noteworthy influence on the electrical response of the analyzed waveguide filters.

ACKNOWLEDGMENT

This work was supported by the Ministerio de Economía y Competitividad, Spanish Government, under the Research Project TEC2013-47037-C5-4-R.

REFERENCES

- [1] U. Balaji, "CAD of resonant circular iris waveguide filter with dielectric filled cavities," *Progress in Electromagnetics Research Symposium Proceedings*, pp. 1139-1141, 1993.

- [2] V. Kesari, "Analysis of alternate dielectric and metal vane loaded circular waveguide for a wideband gyro-TWT," *IEEE Transactions on Electron Devices*, vol. 61, no. 3, pp. 915-920, 2014.
- [3] A. Tribak, J. L. Cano, A. Mediavilla, and M. Boussois, "Octave bandwidth compact turnstile-based orthomode transducer," *IEEE Microwave and Wireless Components Letters*, vol. 20, no. 10, pp. 539-541, 2010.
- [4] A. A. San Blas, F. J. Pérez, J. Gil, F. Mira, V. E. Boria, and B. Gimeno, "Full-wave analysis and design of broadband turnstile junctions," *Progress In Electromagnetics Research Letters*, vol. 24, pp. 149-158, 2011.
- [5] J. Uher, J. Bornemann, and U. Rosenberg, *Waveguide Components for Antenna Feed Systems: Theory and CAD*, Artech House, Norwood, 1993.
- [6] G. Conciauro, M. Guglielmi, and R. Sorrentino, *Advanced Modal Analysis: CAD Techniques for Waveguides Components and Filters*, Wiley, Chichester, 2000.
- [7] M. Qudrat-E-Maula, L. Shafai, and Z. A. Pour, "Dielectric loaded circular waveguide feeds," *16th International Symposium on Antenna Technology and Applied Electromagnetics*, pp. 1-2, 2014.
- [8] J. Li, H. Huang, Z. Zhang, W. Song, H. Shao, C. Chen, and W. Huang, "A novel X-band diplexer based on overmoded circular waveguides for high-power microwaves," *IEEE Transactions on Plasma Science*, vol. 41, no. 10, pp. 2724-2728, 2013.
- [9] Z. Shen and R. H. MacPhie, "Scattering by a thick off-centered circular iris in circular waveguide," *IEEE Transactions on Microwave Theory and Techniques*, vol. 43, no. 11, pp. 2639-2642, 1995.
- [10] K. Wu, "An optimal circular-waveguide dual-mode filter without tuning screws," *IEEE Transactions on Microwave Theory and Techniques*, vol. 47, no. 3, pp. 271-276, 1999.
- [11] S. P. Yeo and S. G. Teo, "Thick eccentric circular iris in circular waveguide," *IEEE Transactions on Microwave Theory and Techniques*, vol. 46, no. 8, pp. 1177-1180, 1998.
- [12] M. Yahia, J. W. Tao, and H. Sakli, "Analysis of complex discontinuities in circular waveguides using hybrid finite element method and multimodal variational method," *Progress In Electromagnetics Research Letters*, vol. 51, pp. 101-107, 2015.
- [13] G. Gerini, M. Guglielmi, and G. Lastoria, "Efficient integral equation formulations for the computation of the multimode admittance or impedance matrix of planar waveguide junctions," *IEEE MTT-S International Microwave Symposium Digest*, pp. 1747-1750, 1998.
- [14] R. R. Mansour and R. H. MacPhie, "An improved transmission matrix formulation of cascaded discontinuities and its application to E-plane circuits," *IEEE Transactions on Microwave Theory and Techniques*, vol. 34, no. 12, pp. 1490-1498, 1986.
- [15] G. G. Gentili, "Properties of TE-TM mode-matching techniques," *IEEE Transactions on Microwave Theory and Techniques*, vol. 39, no. 9, pp. 1669-1673, 1991.
- [16] B. Gimeno and M. Guglielmi, "Multimode equivalent network representation for junctions between coaxial and circular waveguides," *International Journal of Microwave and Millimeter-Wave Computer-Aided Engineering*, vol. 7, no. 2, pp. 180-194, 1997.
- [17] V. E. Boria, G. Gerini, and M. Guglielmi, "An efficient inversion technique for banded linear systems," *IEEE MTT-S International Microwave Symposium Digest*, pp. 1567-1570, 1997.



Ángel A. San-Blas received a M.S. degree and a Ph.D. degree in Telecommunications Engineering, both from the Polytechnic University of Valencia, Valencia (Spain), in 2000 and 2008, respectively. In 2001, he became a Researcher with the Department of Communications, Polytechnic University of Valencia, where he was involved in the development of simulation tools for the full-wave analysis and design of passive waveguide devices. From November 2001 to March 2002, he was a Researcher at Department of Electronics, University of Pavia, Pavia (Italy), in the framework of the European Network MMCODEF (Millimeter-wave and Microwave Components Design Framework for Ground and Space Multimedia Network, V European Framework Programme). Since 2003, he has been an Associate Professor with the Department of Communications Engineering, Miguel Hernández University of Elche, Elche (Spain). His current research interests include numerical methods for the efficient analysis and design of passive and active waveguide components.



José M. Roca received a Telecommunications Engineering degree from the Miguel Hernández University of Elche, Elche (Spain) in 2014. He then joined the Department of Communications Engineering, Miguel Hernández University of Elche, to work on the

development of efficient simulation tools for the analysis and design of microwave and millimeter-wave devices making use of full-wave analysis methods.